Growth and capping of InAs/GaAs quantum dots investigated by X-ray Bragg-surface diffraction

Raul O. Freitas, Alain A. Quivy, and Sérgio L. Morelhão*
Instituto de Física, Universidade de São Paulo, Caixa Postal 66318, CEP 05315-970, São Paulo, SP, Brazil
(Dated: December 16, 2008)

An X-ray diffraction method, based on the excitation of a surface diffracted wave, is described to investigate the capping process of InAs/GaAs (001) quantum dots (QDs). It is sensitive to the tiny misorientation of (111) planes at the surface of the buffer layer on samples with exposed QDs. After capping, the misorientation occurs in the cap-layer lattice faceting the QDs, and its magnitude can be as large as 10° depending on the QDs growth rates, probably due to changes in the size and shape of the QDs. A slow strain release process taking place at room temperature has also been observed by monitoring the misorientation angle of the (111) planes.

PACS numbers: Valid PACS appear here

Self-organized quantum dots (QDs) on semiconductor surfaces are energy-discretizer features for applications in many electronic and optoelectronic devices.[1] Size, shape, and composition are the most important parameters determining the discrete energy levels of charge carriers inside the dots.[2] Minimization of strain during the initial stages of heteroepitaxial growth of lattice mismatched materials plays an essential role in the QDs spontaneous formation,[3,4] but their final parameters also depend on other growth conditions such as temperature and deposition rates.[5] In addition, device processing also requires embedded QDs on the semiconductor matrix, which is achieved by deposition of capping layers. It is an even more complex heteroepitaxial process since faceting, segregation, intermixing, and strain-enhanced diffusion are other phenomena, besides strain release, that also take place at the cap layer/QDs interface and can drastically change the QDs morphology and composition.[4]

To gain knowledge on the mechanisms ruling the atomic arrangements on these nanostructured systems, great efforts have been pulled out in the last few years. Surface probing techniques can provide information of the QDs when they are on top of the exposed surface[6–11] or after covering by just a few monolayers,[4,12] but precise experimental investigation of embedded QD systems in nanometer scale remains challenging.[3,13] Although cross-sectional microscopies are available techniques for high-resolution analysis,[14–16] sample preparation procedures are, in some cases, very time consuming and they are destructive, which compromises time-evolution related studies such as thermal induced atomic interdiffusion and aging processes of the devices. Moreover, these techniques analyze a single QD, or a small number of them that are exposed on the cleaved surface. How representative is this sampling regarding the distribution of QDs determining the optoelectronic properties of the devices and how does the distribution change as a function of the cap-layer growth conditions? These are questions that have not been addressed yet. Therefore, alternative non-destructive techniques able to access average structural information on the total ensemble of embedded QDs can be very helpful in shedding light on the capping process.

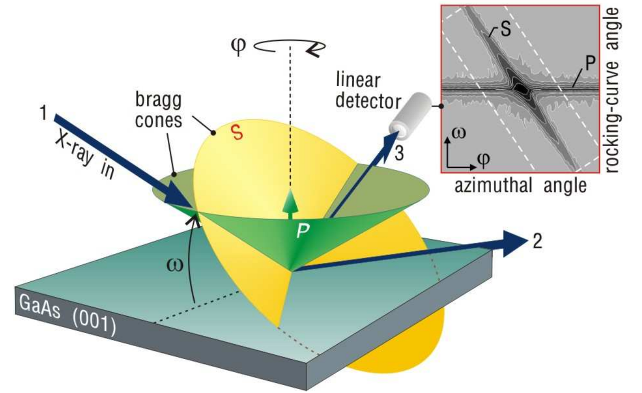

FIG. 1: In single crystals undergoing Bragg-surface diffraction (BSD), rescattering processes of the surface beam 2 provide a well define streak of the S cone when scanning the BSD condition, i.e. the intersection of the P and S Bragg cones, with a collimated monochromatic beam in ordinary diffraction geometry of symmetric Bragg reflections: diffraction cone P, incident beam 1, and diffracted beam 3.

X-ray Bragg-surface diffraction (BSD) is a particular case of 3-beam multiple diffraction where an extremely asymmetric reflection, diffracting nearly parallel to the macroscopic surface of the sample, is excited simultaneously with the symmetric Bragg reflection, Fig. 1. Due to the very grazing angle of the surface beam, any defect at the crystal surface may also increase the rescattering condition, a fact that have been used to investigate surface-finishing and ion-implantation effects on semiconductors[17,18] and, more recently, to directly probe interface strain with atomic resolution in depth on epitaxial films.[19] These unique properties of the BSD make it also very suitable, in principle, to investigate nanostructures on top of semiconductor single crystals. In this work we exploit this potential of the BSD for studying the growth and capping of InAs/GaAs QDs.

Samples were MBE grown on semi-insulating GaAs (100) substrates, with 200 nm GaAs buffer layers de-

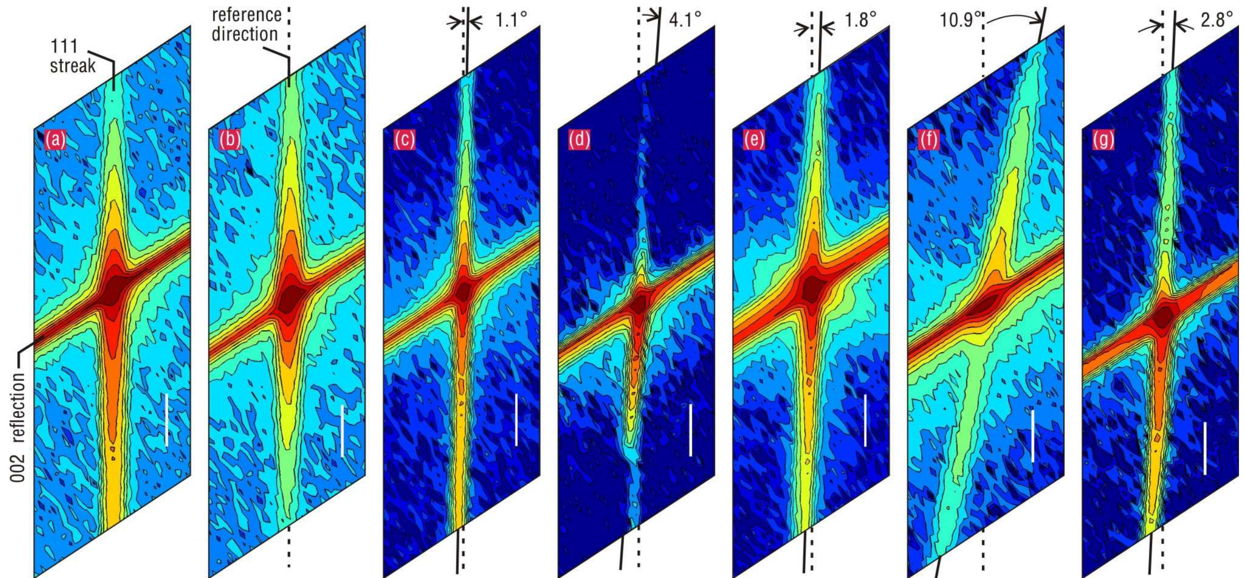

FIG. 2: Two-dimensional intensity profiles of BSD in a series of samples. (a,b) Commercial GaAs (001) wafer before (a) and after (b) 1 μm chemical etching of the surface. (c,d) QDs grown at low rate of 0.007 ML/s: before (c) and after (d) capping. (e,f,g) QDs grown at high rate of 0.09 ML/s: before (e) and after (f) capping, and also the same sample after 1 year (g). White bars stand for 100 arcseconds.

posited at 580 °C.[20] The QDs were formed by deposition of 2.4 monolayers (ML) of InAs at 510 °C and using deposition rates of 0.007 ML/s and 0.09 ML/s. For each deposition rate two samples were prepared: one without capping and another with a 30 nm GaAs cap layer grown at the same substrate temperature of 510 °C. In the samples with no cap layer, densities of 177 QDs/μm^2 and 360 QDs/μm^2 were observed via atomic force microscopy,[21] which implies in an average volume of InAs material per QD of 4.4×10^3 nm^3 and 2.1×10^3 nm^3, for the low (0.007 ML/s) and high (0.09 ML/s) deposition rates, respectively. The monolayer thickness of strained InAs considered when calculating these volumes was 0.325 nm. X-ray data collection have been carried out at diffraction station XRD1, of the Brazilian Synchrotron Light Laboratory (LNLS): bending magnetic beam line, focusing mirror, two-bounce Si (111) monochromator with a sagittal 2nd-crystal, and slit screens. X-ray optics: parallel beam mode (mirror and sagittal-crystal focalized at infinity). Photon energy $E = 9320$ eV, $\Delta E/E \approx 1 \times 10^{-4}$, effective divergences of $18''$ (vertical) $\times$ $24''$ (horizontal), and incident beam size of 0.5×0.5 mm^2. Mechanical accuracy is 0.0002° in both ω and φ rotation axes; see Ref. 22 for more details of the used diffractometer.

In our chosen BSD case, the symmetric Bragg reflection is the 002 reflection, represented by the P Bragg cone in Fig. 1, while the asymmetric 111 reflection, S cone in Fig. 1, is responsible for generating the surface wave. This choice is based on the penetration depth ξ, of the surface wave, which is inversely proportional to its strength. In a general Bragg reflection geometry with diffraction vector $\boldsymbol{G}$, and surface normal direction $\hat{\boldsymbol{n}}$, the penetration depth

$$\xi = \frac{V_c}{4r_e|F(\boldsymbol{G})|}\,\boldsymbol{G}\cdot\hat{\boldsymbol{n}}, \tag{1}$$

is estimated from the extinction depth definition of the dynamical theory of X-ray diffraction (textbooks, e.g. Ref. 23). $V_c = 0.18069$ nm^3 is the GaAs unit cell volume, $r_e = 2.818 \times 10^{-6}$ nm (classical electron radius), and $|F(\boldsymbol{G})| = 146.3$ is the structure factor modulus of the 111 reflection for the used X-ray energy. It provides an intensity attenuation from the entrance crystal surface as $I(z) = I_0 \exp(-\mu_{eff} z)$ where $\mu_{eff} = 2\ln 2/\xi = 7.2 \times 10^{-3}$ nm^{-1} is at least 300 times larger than the photoelectric absorption coefficient in the GaAs crystal. Hence, for asymmetric 111 reflections in (001) samples, even at the incidence angle of the 002 reflection, $\omega = \theta_P = 13.61°$, 50 % of intensity attenuation occurs in less than 100 nm.

Besides the contribution from the 002 reflection, the two-dimensional intensity profile of the BSD also shows a characteristic diagonal streak, the S streak in the inset of Fig. 1, due to the excitation of the 111 reflection. There are two distinct features to be considered: one is the relative orientation of the 111 streak, and the other is the intensity distribution along the streak. The first is ruled by the orientation of the 111 diffracting planes at the sample surface, while the latter depends on rescattering of the surface wave mainly by the crystal-truncation-rod (CTR) of the coupling reflection, the GaAs $\bar{1}\bar{1}1$ reflection in this BSD case. To be used as reference, BSD profiles of a GaAs commercial wafer are shown in Figs. 2(a,b), with the 111 streak aligned vertically. The presence of surface

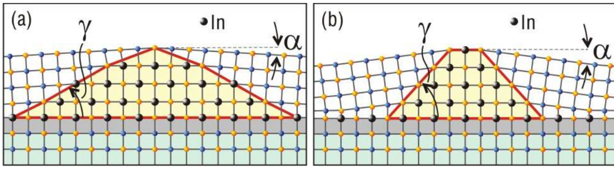

FIG. 3: (a) Perpendicular lattice mismatch at dome-shaped QD / cap-layer interface elastically accommodated by tilting the cap-layer lattice in a few degrees, angle α. (b) In pyramidal QDs, a more accentuated slope angle γ of their facets can induce larger tilt in the surrounding cap-layer lattice.

defects in this wafer is denounced by the slower drop of the streak intensity in the region below the 002 reflection, which has been removed by chemical etching, as can be seen in Fig. 2(b), but no change in the orientation of the streak was noticed. These defects have only enhanced the rescattering of the surface beam when emerging from the crystal ($\Delta\omega = \omega - \theta_P < 0$).

In Figs. 2(c-g), BSD profiles of the samples with freestanding and embedded QDs are shown. The change in the orientation angle of the 111 streak, with respect to the reference one obtained from the GaAs wafer, is indicated above each profile. Small changes are observed in the samples without the cap layer, Figs. 2(c,e). Evidently, the diffracting (111) planes at the buffer layer have been slightly misoriented due to the presence of the freestanding islands. This misorientation as well as the amount of diffuse scattering around the BSD condition are larger in the sample with higher density of small QDs, Fig. 2(e). Since this misorientation has increased with the density of QDs and not with their size, the misoriented planes contributing to the 111 streak are those related to the areas around the QDs and not those lying below them. After capping, Figs. 2(d,f), there is a remarkable change in the orientation of the streak: from 1.1° to 4.1° and from 1.8° to 10.9° for the samples with QDs grown at low and high rates, respectively. The diffracting (111) planes providing the observed streaks are therefore in the cap-layer lattice.

Elastic accommodation of lattice mismatch in heteroeptaxy on sloped interfaces results, in general, in tilted epitaxal-layer lattice. By assuming fully strained QDs with perpendicular lattice constant $a_\perp = 0.650\,\mathrm{nm}$ and facets with slope angle γ, the relationship $\sin(\gamma - \alpha) = (a_{\mathrm{GaAs}}/a_\perp)\sin\gamma$ would give us an estimative on the relative tilt angle α, of the cap-layer lattice when faceting the QDs, as schematized in Fig. 3. For sloped facets by $\gamma \simeq 30°$ and $\gamma \simeq 60°$ the tilt angles are very close to those obtained from the 111 streaks in Figs. 2(d) and 2(f), respectively. In these two cases, the patterns of intensity distribution along the streaks are also different. Due to the fact that the surface wave must be coupled by the CTR of the $\bar{1}\bar{1}1$ reflection, only a fraction of the misoriented (111) planes is able to contribute, hence the magnitude of the tilt angle as well as the facet's slope direction can change the intensity patterns along the streaks.

The strain energy accumulated around the QDs, where the tilted cap-layer lattice met a flat surface, is higher in the case where the facets have larger slope, e.g. Fig.3(b). Some mechanisms can act during or after capping to lower this energy: thermal diffusion of In promoting composition intermixing to smear the sharpness of the lattice mismatched interfaces;[3,8] and flattening of the QDs by strain-induced segregation of In. BSD analysis carried out in the sample with QDs grown at a rate of 0.09 ML/s shows that during capping the strain energy has not been totally lowered and that a significant amount is still stored in the sample. Within the time interval of one year, the 111 streak shifted back 8.1°, to 2.8°, as seen in Fig. 2(g), indicating a further but slow strain-release process taking place at room temperature.

In conclusion, we have demonstrated that X-ray Bragg-surface diffraction (BSD) is a very sensitive tool for studying embedded InAs/GaAs (001) QDs systems. When compared to other X-ray techniques such as grazing incidence diffraction[9,10] and scattering,[11] which have in practice been applied to systems with exposed QDs only, the presented method has a few major advantages: *i)* it probes the influence of the QDs on the surrounding atomic lattices (buffer and cap), making it suitable to investigate the growth and capping processes by extracting an information that no other method has been able to: strain gradings via the relative misalignment of atomic planes at the QDs interfaces; *ii)* a direct data analysis is possible, as the one used here, but structure modeling and simulation of scattering (diffraction) could provide more detailed information on single-buried QDs systems, as well as extend the applicability of the method to multi layered systems;[3,13] and *iii)* its relatively simple diffraction geometry and high signal-to-noise ratio (of the 111 streak) imply that the method is not restricted, in principle, to synchrotron facilities. Moreover, it is feasible for carrying out systematic studies on several samples as a function of growth parameters and post-growth treatments, which is crucial in improving our understanding on theses nanostructured systems. In the series of samples analyzed here, the two-dimensional intensity maps have shown evidences that the capping effects on the QDs also depend on size and shape of the QDs prior to the cap-layer growth, and that the residual level of average strain energy after capping is time dependent, fact that can be further investigated via BSD analysis.

The Brazilian agencies CNPq, CAPES and FAPESP were acknowledged for the financial support of this research.

* morelhao@if.usp.br

[1] D. Bimberg, M. Grundmann, and N. N. Ledentsov, *Quantum Dot Heterostructures* (JohnWiley & Sons, Chicheste, 1999).

[2] H.-C. Chung, Y.-F. Lai, C.-P. Liu, Y.-L. Lai, Y.-C. Fang, and L. Hsu, Appl. Phys. Lett. **92**, 051903 (2008).

[3] M. Yang, S. J. Xu, and J. Wang, Appl. Phys. Lett. **92**, 083112 (2008).

[4] G. Costantini, A. Rastelli, C. Manzano, P. Acosta-Diaz, R. Songmuang, G. Katsaros, O. G. Schmidt, and K. Kern, Phys. Rev. Lett. **96**, 226106 (2006).

[5] Q. Gong, P. Offermans, R. Nötzel, P. M. Koenraad, and J. H. Wolter, Appl. Phys. Lett. **85**, 5697 (2004).

[6] D. Leonard, K. Pond, and P. M. Petroff, Phys. Rev. B **50**, 11687 (1994).

[7] I. Mukhametzhanov, Z. Wei, R. Heitz, and A. Madhukar, Appl. Phys. Lett. **75**, 85 (1999).

[8] I. Kegel, T. H. Metzger, A. Lorke, J. Peis, J. Stangl, G. Bauer, J. M. García, and P. M. Petroff, Phys. Rev. Lett. **85**, 1694 (2000).

[9] T. U. Schülli, M. Sztucki, V. Chamard, T. H. Metzger, and D. Schuh, Appl. Phys. Lett. **81**, 448 (2002).

[10] A. Malachias, S. Kycia, G. Medeiros-Ribeiro, R. Magalhães-Paniago, T. I. Kamins, and R. S. Williams, Phys. Rev. Lett. **91**, 176101 (2003).

[11] I. A. Vartanyants, A. V. Zozulya, K. Mundboth, O. M. Yefanov, M.-I. Richard, E. Wintersberger, J. Stangl, A. Diaz, C. Mocuta, T. H. Metzger, et al., Phys. Rev. B **77**, 115317 (2008).

[12] S. Tonomura and K. Yamaguchia, J. Appl. Phys. **104**, 054909 (2008).

[13] S. Tomić, P. Howe, N. M. Harrison, and T. S. Jones, J. Appl. Phys. **99**, 093522 (2006).

[14] Q. Xie, P. Chen, and A. Madhukar, Appl. Phys. Lett. **65**, 2051 (1994).

[15] R. Otto, H. Kirmse, I. Häusler, W. Neumann, A. Rosenauer, D. Bimberg, and L. Müller-Kirsch, Appl. Phys. Lett. **85**, 4908 (2004).

[16] P. Offermans, P. M. Koenraad, J. H. Wolter, D. Granados, J. M. García, V. M. Fomin, V. N. Gladilin, and J. T. Devreese, Appl. Phys. Lett. **87**, 131902 (2005).

[17] S. L. Morelhão and L. P. Cardoso, J. Appl. Cryst. **29**, 446 (1996).

[18] M. A. Hayashi, S. L. Morelhão, L. H. Avanci, and L. P. Cardoso, Appl. Phys. Lett. **71**, 2614 (1997).

[19] W. C. Sun, H. C. Chang, B. K. Wu, Y. R. Chen, C. H. Chu, S. L. Changa, M. Hong, M. T. Tang, and Y. P. Stetsko, Appl. Phys. Lett. **89**, 091915 (2006).

[20] W. Rudno-Rudziński, G. Sȩk, J. Misiewicz, T. E. Lamas, and A. A. Quivy, J. Appl. Phys. **101**, 073518 (2007).

[21] R. O. Freitas, T. E. Lamas, A. A. Quivy, and S. L. Morelhão, Phys. Stat. Sol. (a) **204**, 2548 (2007).

[22] S. L. Morelhão, J. Synchrotron Radiat. **10**, 236 (2003).

[23] J. Als-Nielsen and D. McMorrow, *Elements of Modern X-ray Physics* (John Wiley & Sons, Chichester, 2001).